Original Article

Differential diagnosis of acute and chronic colitis in mice by optical coherence tomography

Dan Li[1#], Shijie Ding[2#], Manting Luo[3], Jinguo Chen[3], Qiukun Zhang[4], Yijuan Liu[2], Anlan Li[2], Shuncong Zhong[4], Jian Ding[5]

[1]Digestive Department, Union Hospital, Fujian Medical University, Fuzhou, China; [2]Digestive Department, the First Affiliated Hospital of Fujian Medical University, Fuzhou, China; [3]School of Mechanical, Electrical and Information Engineering, Putian University, Putian, China; [4]Laboratory of Optics, Terahertz and Non-Destructive Testing, School of Mechanical Engineering and Automation, Fuzhou University, Fuzhou, China; [5]Digestive Department, Minnan Hospital of the First Affiliated Hospital of Fujian Medical University, Fuzhou, China

Contributions: (I) Conception and design: J Ding, D Li, S Ding, S Zhong; (II) Administrative support: J Ding, S Zhong; (III) Provision of study materials or patients: J Ding, M Luo, J Chen, Q Zhang, Y Liu; (IV) Collection and assembly of data: D Li, S Ding, A Li; (V) Data analysis and interpretation: D Li, S Ding, M Luo, Q Zhang, A Li; (VI) Manuscript writing: All authors; (VII) Final approval of manuscript: All authors.

[#]These authors contributed equally to this work.

Correspondence to: Jian Ding. Digestive Department, Minnan Hospital of the First Affiliated Hospital of Fujian Medical University, Hospital of Quangang District, 2098 South Xiangyun Road, Quangang District, Quanzhou 362800, China. Email: docdingjian@163.com; Shuncong Zhong. Laboratory of Optics, Terahertz and Non-Destructive Testing, School of Mechanical Engineering and Automation, Fuzhou University, Alumni House, Qi Shan Campus of Fuzhou University, 2 Xue Yuan Road, University Town, Fuzhou 350108, China. Email: zhongshuncong@hotmail.com.

Background: The differential diagnosis of acute and chronic colitis remains a common clinical problem. Optical coherence tomography (OCT) is a non-invasive, high-resolution imaging technique that can be used to measure morphological changes in the intestinal wall and estimate intestinal inflammation. We aimed to conduct an *ex vivo* experiment on a mouse model investigate the value of OCT as a tool for the differential diagnosis of acute and chronic colitis.

Methods: Mice were administered dextran sulfate sodium salt (DSS) to construct acute and chronic colitis models. Acutely- and chronically-affected intestinal walls were scanned by OCT, and then the scanned colonic tissue samples were stained with hematoxylin and eosin (HE). Structural and morphological changes indicating inflammation in the intestinal wall were evaluated in the HE sections and OCT images using different parameters. The parameters were used in one-way analysis of variance (ANOVA) to screen for a differential diagnosis of acute or chronic colitis.

Results: For the HE sections, the angle of the mucosal folds, length of the basilar part, and submucosal height and area were statistically significant parameters in the comparisons between the mice with acute colitis and the control-group mice ($P<0.05$). In the comparisons between chronic colitis mice and control-group mice, the angle of the mucosal folds, length of the basilar part, submucosal height and area, muscularis thickness, submucosal height + muscularis thickness, and mucosal thickness were statistically significant parameters ($P<0.05$). Finally, in the comparisons between acute colitis mice and those with chronic colitis, the angle of the mucosal folds, submucosal height and area, muscularis thickness, submucosal height + muscularis thickness, and mucosal thickness were statistically significant parameters ($P<0.05$). For the OCT images, only the length of the basilar part and submucosal height + muscularis thickness were statistically significant parameters between the acute colitis mice and control-group mice ($P<0.05$). The length of the basilar part and submucosal height + muscularis thickness were statistically significant between chronic colitis mice and control-group mice ($P<0.05$). In the comparisons between acute colitis mice and those with chronic colitis, only submucosal height + muscularis thickness was a statistically significant parameter ($P<0.05$).

Conclusions: Certain intestinal wall parameters in OCT can be used to make a differential diagnosis between acute and chronic colitis possible. This study contributes to constructing a potential diagnostic system for evaluating colorectal inflammation using OCT.

Keywords: Acute colitis; chronic colitis; differential diagnosis; intestinal wall; optical coherence tomography (OCT)

Submitted Oct 31, 2021. Accepted for publication Mar 09, 2022.
doi: 10.21037/qims-21-1062
View this article at: https://dx.doi.org/10.21037/qims-21-1062

Introduction

Acute colitis is usually the acute response of the intestinal mucosa to pathogenic factors, such as pathogenic microorganisms, and physical or chemical stimuli. Acute erosions often heal quickly with an appropriate immune response or medication (1). Chronic colitis is not self-limiting and is caused by a variety of persistent pathogenic factors. Affected people must take long-term or even lifelong medication, such as in ulcerative colitis (2). Differential diagnosis is necessary to distinguish acute colitis from chronic colitis or acute relapse of chronic colitis (3). Pathological changes of acute inflammation in the intestinal wall are characterized by mucosal and submucosal edema with neutrophilic infiltration (4), while the changes in chronic colitis are characterized by excessive deposition of collagen fibers and extracellular matrix in the intestinal wall (5). The differential diagnosis of acute versus chronic colitis remains a clinical quandary (6). Colonoscopy with routine biopsy is the gold standard for the diagnosis of inflammatory bowel disease (7); however, colonoscopy cannot accurately provide evidence of excessive deposition of collagen fibers and extracellular matrix in the intestinal wall in real-time (6,8,9). Therefore, patients presenting with acute inflammation are often treated empirically and must wait for a prognosis to be determined during follow-up. Non-invasive, high-resolution imaging technology is necessary to differentiate acute from chronic colitis and acute from acute relapsing chronic colitis, is also useful for assessing histological healing or endoscopic healing.

Optical coherence tomography (OCT) is a recent, rapidly developing, high-definition light imaging technique (10) which can provide orthotropic images by measuring tissue backscattered light to obtain high-resolution cross-sectional tomography images of the microstructure inside biological tissues. It is characterized by its biopsy ability, non-invasiveness, and real-time detection (11,12). The axial resolution of OCT can reach more than 10 times that of endoscopic ultrasound, reaching the micron level (13). It has been used in many fields, including ophthalmology, oncology, cardiovascular medicine, and dermatology, and is emerging as a promising diagnostic modality for gastrointestinal diseases (14-16). From 2004, colonoscopic OCT was reported to be feasible and accurate in detecting disruptions in the layered structure of the colon wall to distinguish ulcerative colitis from Crohn's disease *ex vivo* and *in vivo* (17-20). However, the resolution of the OCT images in these studies required further improvement and lacked relevant parameters for the quantitative analysis of OCT images. In another study, OCT was utilized to quantitatively evaluate the structural changes in the esophagi of rodents with eosinophilic esophagitis (EoE)-like disease (21). Combined with quantitative diagnostic parameters, OCT imaging technology—a non-invasive imaging tool—can be used to improve diagnostic accuracy in gastrointestinal diseases. In our previous work, we confirmed that OCT could be used to detect acute colitis and evaluate the degree of inflammation in colitis using specific parameters (22), providing an excellent positive detection rate and diagnostic accuracy for differentiating between early colorectal dysplasia and cancer (23). In the present study, OCT was evaluated as a tool in the differential diagnosis of acute and chronic colitis *ex vivo*. We present the following article in accordance with the Animal Research: Reporting of In Vivo Experiments (ARRIVE) reporting checklist (available at https://qims.amegroups.com/article/view/10.21037/qims-21-1062/rc).

Methods

Animals and materials

Healthy female BALB/c mice (6–8 weeks old; 18–22 g) were purchased from Wu's Experimental Animal Center (Minhou

Table 1 DAI (25)

Weight loss rate (%)	Stool consistency	Stool bleeding	Scoring
0	Normal	Normal	0
0–5	–	–	1
5–10	Loose	Occult blood positive	2
10–15	–	–	3
>15	Diarrhea	Hematochezia	4

Normal stool: formed stool, normal color; loose stool: pasty and semi-formed stool that does not adhere to the anus; diarrhea stool: unformed, very watery stool that can adhere to the anus. DAI, disease activity index.

Table 2 Histological scoring criteria for inflammatory intestinal injury (26)

Neutrophil grade	Lesion depth	Crypt destruction	Lesion area	Scoring
None	None	None	0	0
<10 cells/high magnification lens	Mucosal layer	Basal 1/3 crypt	1–25%	1
10–50 cells/high magnification lens	Submucosa	Basal 2/3 crypt	26–50%	2
>50 cells/high magnification lens	Muscularis	Only intact surface epithelium	51–75%	3
Obvious acute inflammation with ulcer formation	Serosa layer	All crypts and epithelium destroyed	76–100%	4

0–3 indicates normal without inflammation; 4–6 indicates mild inflammation; 7–10 indicates moderate inflammation; and 11–14 indicates severe inflammation.

County, Fuzhou, China). The animals were housed in cages, with 6 mice per cage, at 25 ℃ with a relative humidity of 60%±10% and a 12-h light/dark cycle. All experiments were performed under a project license granted by the Institutional Animal Care and Use Committee (IACUC) of Fujian Medical University (No. FJMU IACUC 2019-0069), in compliance with IACUC institutional guidelines for the care and use of animals.

Models of acute and chronic dextran sulfate sodium salt (DSS)-induced colitis

Mice were randomly divided into a control group (10 mice), an acute colitis group (12 mice), and a chronic colitis group (12 mice). Mice in the acute colitis group were fed with freshly prepared 3.0% chronic DSS ad libitum for 7 days. Mice in the chronic colitis group were exposed to 3 cycles of DSS. In each cycle, the mice were fed with freshly prepared DSS ad libitum for 7 days, then distilled water for 14 days.

Weight loss and intestinal bleeding were observed and recorded for all mice at least 3 times per week (24).

Disease activity index (DAI)

The DAI is a standard scoring system comprising degrees of weight loss and intestinal bleeding (25). The DAI scores range from 0 to 12 (total score). The specific content of the scoring criteria is shown in *Table 1*.

Histological analysis

Intestinal sections were scanned by OCT, and then the scanned colonic tissue samples were stained with hematoxylin and eosin (HE). Histopathological changes in the intestinal mucosa were measured using a double-blind method. The inflammatory histological injury score criteria for evaluating the degree of colorectal inflammation and the specific content of the scoring criteria are shown in *Table 2* (26).

OCT image acquisition and data processing

OCT scanning

Mice with DSS-induced colitis were fasted for 12 h for solid food and 6 h for water before being sacrificed by isoflurane

inhalational anesthesia. Their colons were removed, and colorectal tissues 2 cm from the anal margin with a length of 0.5 cm were removed, cut open lengthwise, rinsed with saline, and, after drying on filter paper, placed on glass slides. Samples were then placed in the scanning window for OCT evaluation.

A GAN220 spectral-domain OCT (SD-OCT) system (Thorlabs, Newton, NJ, USA) was used for scanning (central wavelength: 930 nm; axial resolution: 2.85 μm; lateral resolution: 2.82 μm; axial scan line frequency: 5.5–36 kHz). The three-dimensional (3D) OCT images were obtained by instantaneous uniaxial imaging using the probe light and X-Y two-dimensional (2D) scanning of the biaxial galvanometer. The Z-axis resolution and imaging depth of the OCT system were fixed at 2.85 μm and 2.9 mm (847 pixels), respectively. The range and resolution of the X-Y plane were determined by the scanning amplitude and scanning speed of the galvanometer. In this experiment, the imaging range and resolution of the X-axis were 4.52 mm (512 pixels) and 8.8 μm, respectively, and the imaging range and resolution of the Y-axis were 4.08 mm (67 pixels) and 60.9 μm, respectively. The working distance of the probe was fixed so that when the sample was correctly placed under the probe, a 3D OCT image could be obtained. As samples of different materials have different back-reflected light intensities, better image quality was obtained by adjusting the light intensity of the reference arm. Optimum intensity for the reference light was adjusted by opening or closing the variable aperture of the OCT.

Data processing procedures

All OCT image analyses were performed using custom routines written in MATLAB (Mathworks, Inc., Natick, MA, USA). The HE-stained pathological sections were analyzed using a light microscope (Olympus CX41; Olympus Corp., Tokyo, Japan), and quantitative data were analyzed using Image-Pro Plus 6.0.0260 (Media Cybernetics Inc., Silver Spring, MD, USA).

Data analysis

Colorectal tissues 2 cm away from the anal margin were selected, and a length of 0.5 cm was scanned by the OCT image system to obtain multiple OCT images. One OCT image was randomly selected along with the matched HE-stained section for statistical analysis. The mucosal morphological diagnostic parameters of both the OCT images and HE-stained pathology images were measured by 3 double-blinded investigators, and the average of the 3 measurements for each image was calculated. The mucosal morphological changes in the mice with acute and chronic colitis were assessed by these parameter indices. The difference in the mean values between groups was compared to determine statistical significance. Measurement data were represented as the mean ± standard deviation (SD), and one-way analysis of variance (ANOVA) was used to compare between groups. The least significance difference (LSD) method was used when assuming homogeneity of variance. If the homogeneity of variance was not satisfied, the Games-Howell method (applicable to non-assumed homogeneity of variance) was used. A P value <0.05 was considered statistically significant.

Results

The construction of colitis mouse model

Acute colitis mouse model

The mice in the acute colitis group gradually developed lethargy, loose stools, occasional diarrhea, and loss of body weight from the third day of 3% DSS administration. Symptoms gradually progressed to listlessness, arched backs, decreased appetite, and a sharp decrease in body mass index (BMI), with manifestations of intestinal inflammation, such as diarrhea and gross bloody stools. The DAI peaked on day 7 (*Figure 1*).

Chronic colitis mouse model

Inflammation in the chronic colitis group peaked on day 7 of modeling in the first cycle. When the mice were fed distilled water, their mental status and symptoms gradually improved. The DAI decreased, and body weight returned gradually in the 7 days after DSS withdrawal, and the disease activity disappeared after 14 days. In the last 2 cycles, diarrhea and gross bloody stools appeared earlier than during the first cycle, and soft stools or diarrhea persisted even after drug withdrawal (*Figure 2*).

OCT images of the intestinal wall

The different intestinal wall layers were identified with OCT, displayed as differences in the backscattered reflection intensity that presented in a faint stripe-like pattern. The intestinal mucosal epithelium was the first bright layer, consisting of epithelial cells with high scattering (*Figure 3*). From the mucosa to the lamina propria and

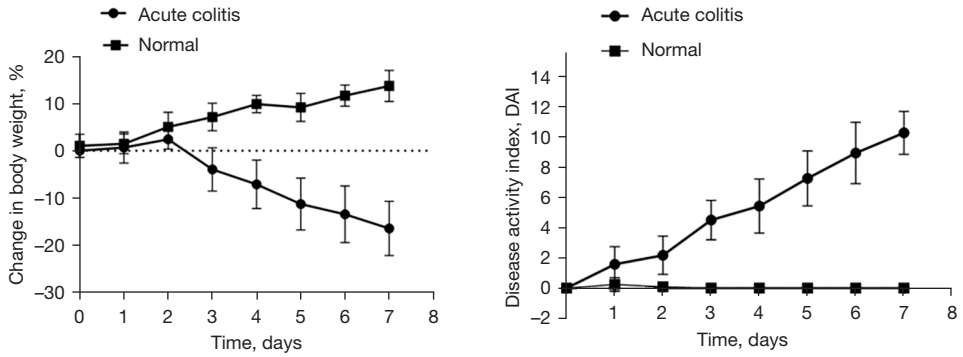

Figure 1 Changes in body weight and DAI in the acute colitis group, as compared with the control group (P<0.05). DAI, disease activity index.

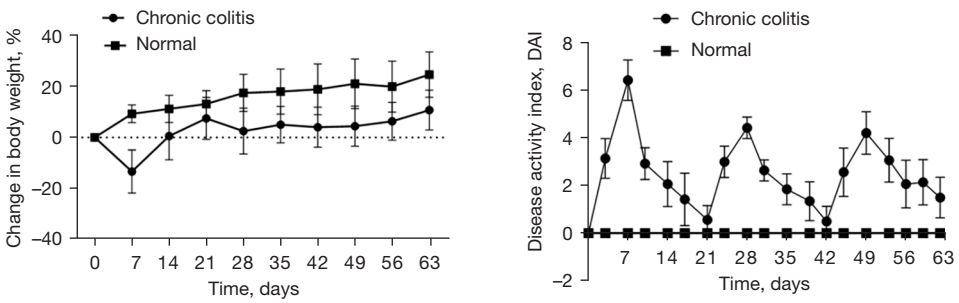

Figure 2 Changes in body weight and DAI in the chronic colitis group, as compared with the control group (P<0.05). DAI, disease activity index.

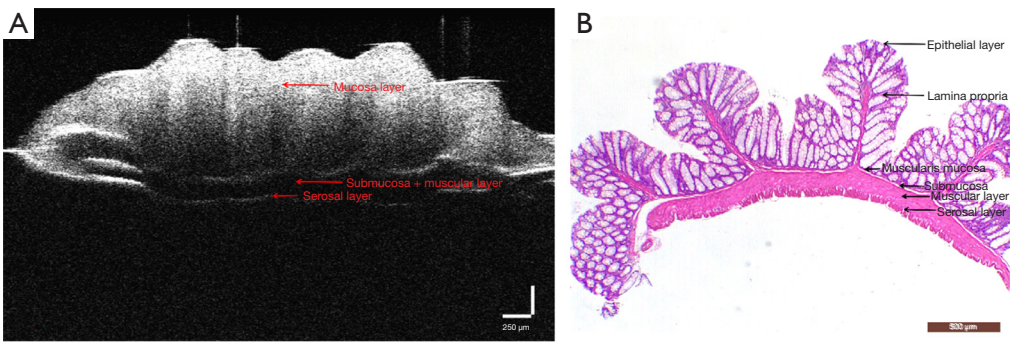

Figure 3 The layers of normal colon tissue presented in different images. (A) OCT image of normal colonic tissue. The different layers are distinguished by relative differences in the intensity of the backscattering. (B) The corresponding histological image (stained with HE). OCT, optical coherence tomography; HE, hematoxylin and eosin.

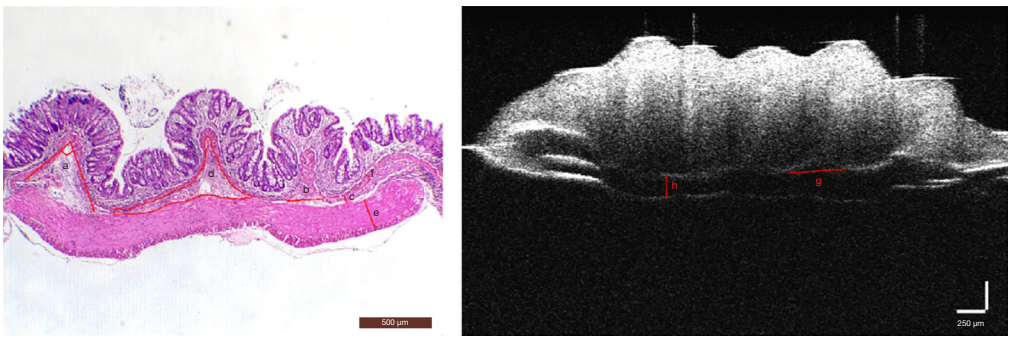

Figure 4 The parameters for the indices of chronic colitis in HE-stained pathological sections from (a) to (f) (left image): (a) angle of the mucosal folds (°); (b) length of the basilar part (μm); (c) submucosal height (μm); (d) submucosal area (μm^2); (e) muscularis thickness (μm); and (f) muscularis mucosa thickness (μm). (c,e): submucosal height + muscularis thickness (μm). The OCT image on the right indicates the parameters for the indices of chronic colitis; (g) length of the basilar part (μm); (h) submucosal height + muscularis thickness (μm). HE, hematoxylin and eosin; OCT, optical coherence tomography.

muscularis mucosa, the reflection intensity became weaker until reaching the boundary of the muscularis mucosa. The boundary between the muscularis mucosa and the submucosa was a low-brightness reflective streak with weak scattering. The submucosa and muscularis could not be distinguished by OCT. The serosa was the deepest layer of the intestinal lumen and appeared as a low-brightness reflective streak.

Parameters for evaluating colitis in the HE-stained pathological sections and OCT images

According to the changes in the morphological structure of the intestinal wall, 6 diagnostic parameters based on the HE pathological sections and 2 diagnostic parameters based on the OCT images were evaluated according to their ability to indicate the degree of inflammation. The specific parameters can be seen in *Figure 4*, and specific details regarding the measurement of these parameters can be found in our prior research (22). We observed 2D and 3D OCT images of mice with acute and chronic colitis to evaluate the morphological structural changes in acute and chronic colitis (*Figure 5*).

Statistical analysis

For the HE sections, the angle of the mucosal folds, length of the basilar part, and submucosal height and area were statistically significant parameters in the comparisons between the acute colitis and control groups ($P<0.05$). In the comparisons between the chronic colitis and control groups, the angle of the mucosal folds, length of the basilar part, submucosal height and area, muscularis thickness, submucosal height + muscularis thickness, and muscularis mucosa thickness were statistically significant parameters ($P<0.05$), and in the comparisons between the acute and chronic colitis groups, the angle of the mucosal folds, submucosal height and area, muscularis thickness, submucosal height + muscularis thickness, and muscularis mucosa thickness were statistically significant parameters ($P<0.05$). The parameters for the HE-stained sections are shown in more detail in *Table 3*.

For the OCT images, the length of the basilar part and submucosal height + muscularis thickness were statistically significant parameters in the comparisons between the acute colitis and control groups ($P<0.05$). In comparisons between the chronic colitis and control groups, the length of the basilar part and submucosal height + muscularis thickness were statistically significant parameters ($P<0.05$). Finally, only submucosal height + muscularis thickness was statistically significant in the comparisons between the acute and chronic colitis groups ($P<0.05$). The parameters for the OCT images are shown in more detail in *Table 4*.

Discussion

In acute colitis, mucosal edema occurs with marked neutrophilic infiltration and inflammatory cytokine secretion, causing vascular endothelial dilatation and the accumulation of a large amount of exudate in the submucosa, followed by morphological and structural changes in the mucosa and submucosa (27). Mucosal edema

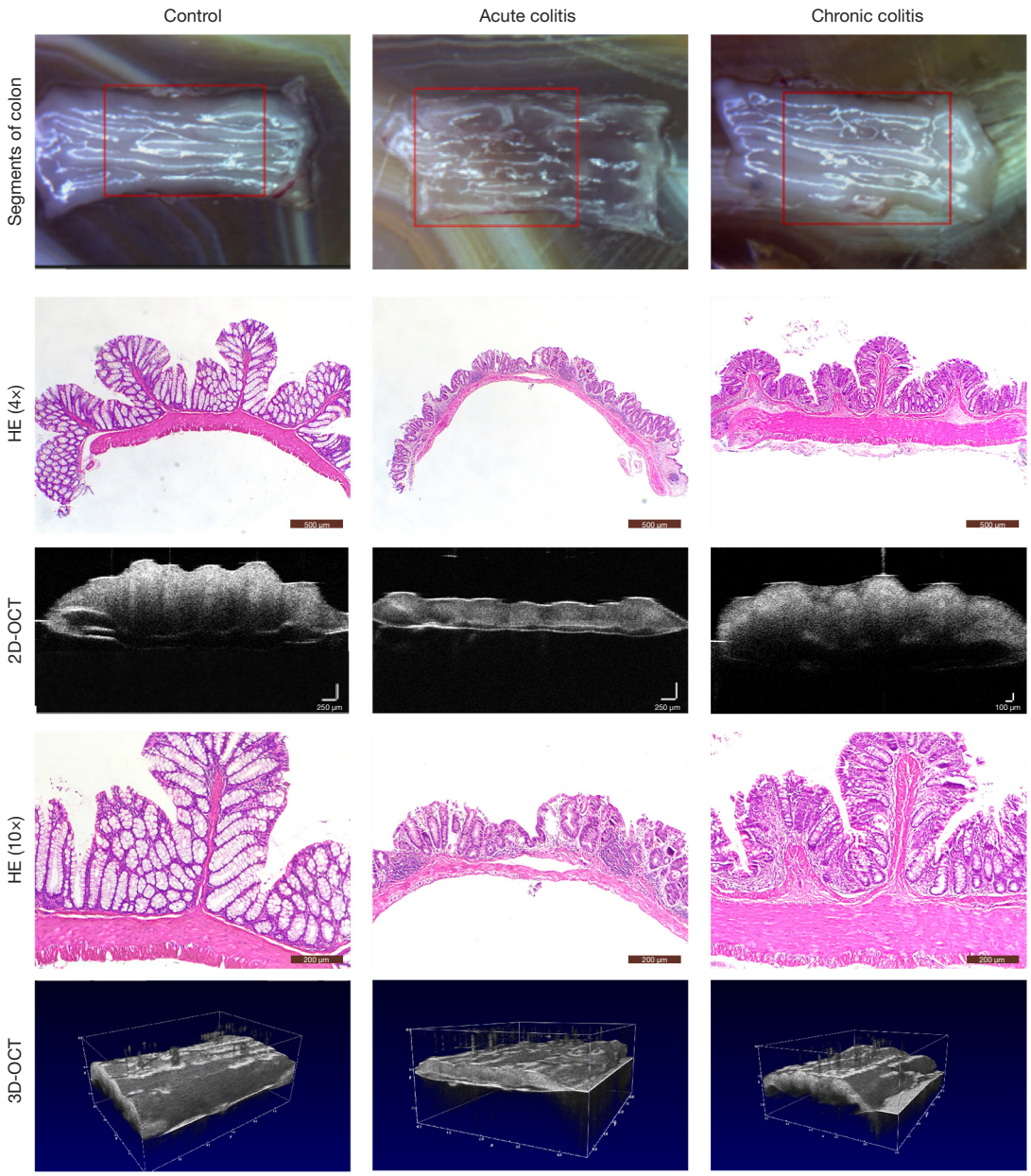

Figure 5 2D and 3D OCT images of acute and chronic colitis. HE-stained pathological section images were matched to the OCT morphological and structural characteristics. 2D, two-dimensional; 3D, three-dimensional; OCT, optical coherence tomography; HE, hematoxylin and eosin.

related to acute inflammation is often limited to the mucosa and submucosa, with the muscularis rarely involved (28). However, the intestinal wall in chronic inflammation undergoes recurrence and remission of inflammation, and chronic hyperplasia-like changes appear in the intestinal wall (29). In chronic inflammation, the structure of the mucosal crypts is destroyed and deformed, the glands atrophy, and lymphocyte infiltration is accompanied by a large amount of extracellular matrix deposition and fibrous tissue hyperplasia (30). The proliferation of intestinal tissue eventually leads to thickening of the intestinal wall and narrowing of the intestinal lumen (31).

Table 3 Parameters for the HE-stained sections

Dependent variable	Type of inflammation	HE picture (sheets)	Mean ± SD	P value	
				Acute	Chronic
Angle of mucosal folds (°)	Normal	10	9.35±3.31	0.000	0.000
	Acute	12	123.39±20.18		0.000
	Chronic	12	58.60±12.87		
Length of basilar part (μm)	Normal	10	65.56±13.50	0.000	0.000
	Acute	12	380.65±85.42		0.071
	Chronic	12	467.78±96.37		
Submucosal height (μm)	Normal	10	22.10±4.29	0.004	0.002
	Acute	12	48.95±8.47		0.009
	Chronic	12	126.06±26.89		
Submucosal area (μm^2)	Normal	10	7,792.78±3,076.65	0.004	0.000
	Acute	12	28,117.70±16,645.02		0.011
	Chronic	12	117,814.20±84,031.19		
Muscularis thickness (μm)	Normal	10	129.72±24.86	0.387	0.000
	Acute	12	115.52±24.25	0.000	
	Chronic	12	272.87±25.07		
Submucosal height + muscularis thickness (μm)	Normal	10	151.82±25.10	0.538	0.000
	Acute	12	164.47±29.91	0.000	
	Chronic	12	398.93±43.24		
Muscularis mucosa thickness	Normal	10	12.52±2.08	0.653	0.000
	Acute	12	13.51±3.10		0.000
	Chronic	12	46.97±7.18		

Differences in the mean values between groups were compared to determine statistical significance. Measurement data are represented as the mean ± SD, and one-way ANOVA was used to compare between groups. The significance level was set at α=0.05, and differences were considered significant when P<0.05. HE, hematoxylin and eosin; SD, standard deviation; ANOVA, analysis of variance.

Table 4 Parameters for the OCT images

Dependent variable	Type of inflammation	OCT image (sheets)	Mean ± SD	P value	
				Acute	Chronic
Length of basilar part (μm)	Normal	10	233.46 ±37.92	0.000	0.000
	Acute	12	562.02±106.39		0.265
	Chronic	12	635.56±114.92		
Submucosal height + muscularis thickness (μm)	Normal	10	192.19±53.06	0.036	0.000
	Acute	12	138.78±31.97		0.000
	Chronic	12	505.38±45.53		

Differences in the mean values between groups were compared to determine statistical significance. Measurement data are represented as the mean ± SD, and one-way ANOVA was used to compare between groups. The significance level was set at α=0.05, and the differences were considered significant when P<0.05. OCT, optical coherence tomography; SD, standard deviation; ANOVA, analysis of variance.

In this study, we successfully constructed mouse models of acute and chronic colitis and evaluated the pathological changes in the intestinal wall morphology using HE sections and OCT images. We then performed the diagnosis and differential diagnosis of acute and chronic inflammation of the intestine. For the HE sections, 4 parameters (the angle of the mucosal folds, length of the basilar part, and submucosal height and area) increased significantly in the acute colitis group relative to changes in the control group. These results were consistent with our previous study (22). Pathological morphological changes are the result of acute mucosal edema and neutrophilic infiltration. In the chronic colitis group, 7 parameters (the angle of the mucosal folds, length of the basilar part, submucosal height and area, muscularis thickness, submucosal height + muscularis thickness, and muscularis mucosa thickness) increased statistically, relative to changes in the control group. The differences were due to matrix deposition and fibrous hyperplasia in the intestinal wall during continuous recurrence and remission of inflammation. These pathological changes dominated the differences between acute and chronic colitis. Among these 7 parameters, submucosal height, length of the basilar part, submucosal area, muscularis thickness, submucosal thickness + muscularis thickness, and muscularis mucosa thickness changed significantly in the chronic colitis group, relative to changes in the acute colitis group, due to more severe and recurrent inflammation. However, interestingly, the angle of the mucosal folds decreased significantly in the chronic colitis group, which may be due to acute inflammation recovery and mucosal dehydration.

The parameters for the HE-stained sections provided the basis for evaluating the OCT images. Because the submucosa and the mucosa of the intestinal wall were dark layers, and the boundary between the 2 layers was unclear, we were unable to observe morphological structural changes of the submucosa in the OCT images. Therefore, we had previously established only 2 diagnostic parameters for OCT scanning—length of the basilar part and submucosal height + muscularis thickness—to evaluate acute inflammation in the intestinal wall (22). In the current study, these 2 parameters also significantly increased in the chronic colitis group, relative to changes in the control group. However, the most meaningful result was that submucosal height + muscularis thickness increased significantly in the chronic colitis group, relative to changes in the acute colitis group. This confirmed that these parameters can be used in OCT scanning for the differential diagnosis of acute and chronic colitis. The increased parameter values in the chronic colitis group can be explained by the increased thickness of both the submucosa and muscularis with long-term and recurrent inflammation owing to matrix deposition and fibrous hyperplasia. Although OCT cannot distinguish an exact boundary between the 2 layers or determine which layer dominates the increased thickness, the results of the HE section analysis, as supplementary evidence, showed that both submucosal and muscularis layer thickness increased in the chronic colitis group, relative to changes in the acute colitis group. Therefore, submucosal height + muscularis thickness can be measured as a single layer to differentiate between acute and chronic inflammation.

Conclusions

In summary, OCT imaging, as a non-invasive, high-resolution imaging technique, provides a new method for the differential diagnosis of acute and chronic colitis by scanning *in situ* tissue images of intestinal lesions. It can conduct wide-range scanning and evaluate structural changes in the colon wall in a short period. Because of the advantages of high-resolution, biopsy ability, non-invasiveness, and real-time detection, using OCT parameters helps differentiate between acute and chronic colitis, acute or acute relapse of chronic colitis, and histological or endoscopic healing much more conveniently. The OCT can be integrated into a wide range of imaging transmission systems and imaging probes and applied in combination with endoscopy and laparoscopy for *in vivo* detection of gastrointestinal diseases. With advances in endoscopic technology and the miniaturization of OCT imaging devices, this imaging modality will likely become useful in detecting gastrointestinal diseases. Therefore, OCT imaging technology can be utilized to construct a new diagnosis system for intestinal diseases and, more specifically, for inflammatory bowel diseases.

Acknowledgments

We thank Stephanie Knowlton, PhD. from Liwen Bianji, Edanz Editing China for editing the English text of a draft of this manuscript.

Funding: The study was supported by the Natural Science Foundation of Fujian Province (No. 2019J01437); the Quanzhou Science Project of Production, Study, and Investigation (No. WTTJJH-DJ2021); the Fujian Natural Science Foundation (No. 2018J01314); the Joint Funds for

the Innovation of Science and Technology, Fujian Province (No. 2017Y9048); and the Key Clinical Specialty Discipline Construction Program of Fujian, China (Min Wei Ke Jiao, 2012; No. 149).

Footnote

Reporting Checklist: The authors have completed the ARRIVE reporting checklist. Available at https://qims.amegroups.com/article/view/10.21037/qims-21-1062/rc

Conflicts of Interest: All authors have completed the ICMJE uniform disclosure form (available at https://qims.amegroups.com/article/view/10.21037/qims-21-1062/coif). The authors have no conflicts of interest to declare.

Ethical Statement: The authors are accountable for all aspects of the work in ensuring that questions related to the accuracy or integrity of any part of the work are appropriately investigated and resolved. All experiments were performed under a project license (No. FJMU IACUC 2019-0069) granted by the Institutional Animal Care and Use Committee (IACUC) of the Fujian Medical University, in compliance with IACUC institutional guidelines for the care and use of animals.

References

1. Nostrant TT, Kumar NB, Appelman HD. Histopathology differentiates acute self-limited colitis from ulcerative colitis. Gastroenterology 1987;92:318-28.
2. Rogler G. Chronic ulcerative colitis and colorectal cancer. Cancer Lett 2014;345:235-41.
3. Bressenot A, Salleron J, Bastien C, Danese S, Boulagnon-Rombi C, Peyrin-Biroulet L. Comparing histological activity indexes in UC. Gut 2015;64:1412-8.
4. Bersudsky M, Luski L, Fishman D, White RM, Ziv-Sokolovskaya N, Dotan S, Rider P, Kaplanov I, Aychek T, Dinarello CA, Apte RN, Voronov E. Non-redundant properties of IL-1α and IL-1β during acute colon inflammation in mice. Gut 2014;63:598-609.
5. Latella G, Di Gregorio J, Flati V, Rieder F, Lawrance IC. Mechanisms of initiation and progression of intestinal fibrosis in IBD. Scand J Gastroenterol 2015;50:53-65.
6. Calafat M, Lobatón T, Hernández-Gallego A, Mañosa M, Torres P, Cañete F, Cabré E, Ojanguren I, Domènech E. Acute histological inflammatory activity is associated with clinical relapse in patients with ulcerative colitis in clinical and endoscopic remission. Dig Liver Dis 2017;49:1327-31.
7. Iacucci M, Furfaro F, Matsumoto T, Uraoka T, Smith S, Ghosh S, Kiesslich R. Advanced endoscopic techniques in the assessment of inflammatory bowel disease: new technology, new era. Gut 2019;68:562-72.
8. Hamilton MJ. The valuable role of endoscopy in inflammatory bowel disease. Diagn Ther Endosc 2012;2012:467979.
9. Bryant RV, Burger DC, Delo J, Walsh AJ, Thomas S, von Herbay A, Buchel OC, White L, Brain O, Keshav S, Warren BF, Travis SP. Beyond endoscopic mucosal healing in UC: histological remission better predicts corticosteroid use and hospitalisation over 6 years of follow-up. Gut 2016;65:408-14.
10. Carrasco-Zevallos OM, Viehland C, Keller B, Draelos M, Kuo AN, Toth CA, Izatt JA. Review of intraoperative optical coherence tomography: technology and applications [Invited]. Biomed Opt Express 2017;8:1607-37.
11. Kołodziej A, Krajewski W, Matuszewski M, Tupikowski K. Review of current optical diagnostic techniques for non-muscle-invasive bladder cancer. Cent European J Urol 2016;69:150-6.
12. Jelvehgaran P, de Bruin DM, Khmelinskii A, Borst G, Steinberg JD, Song JY, de Vos J, van Leeuwen TG, Alderliesten T, de Boer JF, van Herk M. Optical coherence tomography to detect acute esophageal radiation-induced damage in mice: A validation study. J Biophotonics 2019;12:e201800440.
13. Hatta W, Uno K, Koike T, Iijima K, Asano N, Imatani A, Shimosegawa T. A prospective comparative study of optical coherence tomography and EUS for tumor staging of superficial esophageal squamous cell carcinoma. Gastrointest Endosc 2012;76:548-55.
14. Shen B, Zuccaro G Jr. Optical coherence tomography in the gastrointestinal tract. Gastrointest Endosc Clin N Am 2004;14:555-71, x.
15. Nair A, Liu CH, Singh M, Das S, Le T, Du Y, Soomro S,

Aglyamov S, Mohan C, Larin KV. Assessing colitis ex vivo using optical coherence elastography in a murine model. Quant Imaging Med Surg 2019;9:1429-40.
16. Familiari L, Strangio G, Consolo P, Luigiano C, Bonica M, Barresi G, Barresi V, Familiari P, D'Arrigo G, Alibrandi A, Zirilli A, Fries W, Scaffidi M. Optical coherence tomography evaluation of ulcerative colitis: the patterns and the comparison with histology. Am J Gastroenterol 2006;101:2833-40.
17. Consolo P, Strangio G, Luigiano C, Giacobbe G, Pallio S, Familiari L. Optical coherence tomography in inflammatory bowel disease: prospective evaluation of 35 patients. Dis Colon Rectum 2008;51:1374-80.
18. Shen B, Zuccaro G, Gramlich TL, Gladkova N, Lashner BA, Delaney CP, Connor JT, Remzi FH, Kareta M, Bevins CL, Feldchtein F, Strong SA, Bambrick ML, Trolli P, Fazio VW. Ex vivo histology-correlated optical coherence tomography in the detection of transmural inflammation in Crohn's disease. Clin Gastroenterol Hepatol 2004;2:754-60.
19. Ahsen OO, Liang K, Lee HC, Giacomelli MG, Wang Z, Potsaid B, Figueiredo M, Huang Q, Jayaraman V, Fujimoto JG, Mashimo H. Assessment of Barrett's esophagus and dysplasia with ultrahigh-speed volumetric en face and cross-sectional optical coherence tomography. Endoscopy 2019;51:355-9.
20. Ding Q, Deng Y, Yu X, Yuan J, Zeng Z, Mu G, Wan X, Zhang J, Zhou W, Huang L, Yao L, Gong D, Chen M, Zhu X, Liu L, Yu H. Rapid, High-Resolution, Label-Free, and 3-Dimensional Imaging to Differentiate Colorectal Adenomas and Non-Neoplastic Polyps With Micro-Optical Coherence Tomography. Clin Transl Gastroenterol 2019;10:e00049.
21. Alex A, Noti M, Wojno ED, Artis D, Zhou C. Characterization of eosinophilic esophagitis murine models using optical coherence tomography. Biomed Opt Express 2014;5:609-20.
22. Ding J, Lin J, Li Q, Chen X, Chen W, Zhang Q, He S, Wu T, Wang C, Zhong S, Li D. Optical coherent tomography to evaluate the degree of inflammation in a mouse model of colitis. Quant Imaging Med Surg 2020;10:945-57.
23. Ding J, Li Q, Lin J, He S, Chen W, He Q, Zhang Q, Chen J, Wu T, Zhong S, Li D. Optical coherence tomography for the early detection of colorectal dysplasia and cancer: validation in a murine model. Quant Imaging Med Surg 2021;11:371-9.
24. Wirtz S, Popp V, Kindermann M, Gerlach K, Weigmann B, Fichtner-Feigl S, Neurath MF. Chemically induced mouse models of acute and chronic intestinal inflammation. Nat Protoc 2017;12:1295-309.
25. Sha T, Igaki K, Yamasaki M, Watanabe T, Tsuchimori N. Establishment and validation of a new semi-chronic dextran sulfate sodium-induced model of colitis in mice. Int Immunopharmacol 2013;15:23-9.
26. Madsen KL, Doyle JS, Tavernini MM, Jewell LD, Rennie RP, Fedorak RN. Antibiotic therapy attenuates colitis in interleukin 10 gene-deficient mice. Gastroenterology 2000;118:1094-105.
27. Medzhitov R. Origin and physiological roles of inflammation. Nature 2008;454:428-35.
28. Sairenji T, Collins KL, Evans DV. An Update on Inflammatory Bowel Disease. Prim Care 2017;44:673-92.
29. Gong X, Xu X, Lin S, Cheng Y, Tong J, Li Y. Alterations in biomechanical properties and microstructure of colon wall in early-stage experimental colitis. Exp Ther Med 2017;14:995-1000.
30. Langner C, Aust D, Ensari A, Villanacci V, Becheanu G, Miehlke S, Geboes K, Münch A; Working Group of Digestive Diseases of the European Society of Pathology (ESP) and the European Microscopic Colitis Group (EMCG). Histology of microscopic colitis-review with a practical approach for pathologists. Histopathology 2015;66:613-26.
31. de Bruyn JR, Meijer SL, Wildenberg ME, Bemelman WA, van den Brink GR, D'Haens GR. Development of Fibrosis in Acute and Longstanding Ulcerative Colitis. J Crohns Colitis 2015;9:966-72.

Cite this article as: Li D, Ding S, Luo M, Chen J, Zhang Q, Liu Y, Li A, Zhong S, Ding J. Differential diagnosis of acute and chronic colitis in mice by optical coherence tomography. Quant Imaging Med Surg 2022;12(6):3193-3203. doi: 10.21037/qims-21-1062

